

P-11-10

Pulsating Tension Fatigue Testing of Single and Poly-Crystalline Silicon Microstructures for Silicon MEMS

Takahiro Namazu, Yuji Nagai, and Shozo Inoue

Department of Mechanical and System Engineering, University of Hyogo
2167 Shosha, Himeji, Hyogo 671-2201, Japan
Phone: +81-79-267-4962 E-mail: namazu@eng.u-hyogo.ac.jp

1. Introduction

Single-crystalline silicon (SCS) and poly-crystalline silicon (PCS) are the most dominant structural materials used in microelectromechanical systems (MEMS). MEMS devices, such as accelerometers, pressure sensors, and optical scanners, often include elastically deformable micro-scale hinge structures made of SCS or PCS to generate mechanical cyclic movements. During operation, the silicon micro-components are routinely subjected to fluctuating mechanical stresses, which lead to fatigue damage accumulation that results in premature failure of the micro-components. Hence evaluating and understanding fatigue damage behavior as well as quasi-static mechanical properties of microscale silicon structures are critical for the safe and reliable design of high-performance silicon MEMS devices [1]-[2].

The objective of this work is to investigate the fatigue damage characteristics of microscale SCS and PCS specimens by means of pulsating tension fatigue testing.

2. Experimental Procedure

Specimen

Fig. 1 shows photograph of microscale SCS and PCS specimens for the fatigue tests. All the specimens were fabricated using conventional MEMS techniques. The gauge section of a specimen has a straight shape supported by two SCS blocks with a square hole for mechanical chucking. The nominal dimensions of the gauge section having a rectangular cross-section, formed by deep reactive ion etching, were 60 μm in width, 600 μm in length, and 2 μm in thickness. The PCS specimens deposited by low-pressure chemical vapor deposition possessed a poly-crystal configuration, whereas the SCS specimens were oriented along the [110] direction in the (001) plane, which corresponds to the principal stress direction during testing. Only specimens with dimensional tolerances within $\pm 5\%$ for all dimensions were subjected to cyclic loading tests.

Fatigue Tester

Fig. 2 shows the handmade uniaxial tensile tester. The tester consists of a piezoelectric actuator built in the actuator case, a linear variable differential transformer (LVDT), a load cell, and specimen holders [3]. The actuator applies tensile force to the specimen, hooked on the specimen holders, via a hinge structure. The load cell has an accuracy of 0.10% of full scale: 10 N. The LVDT, which has a resolution of 3 nm, measures relative displacement between specimen holders.

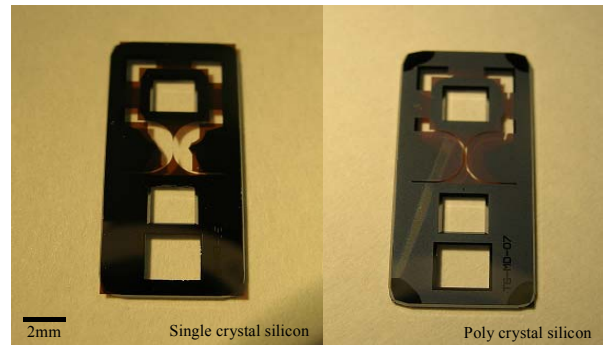


Fig. 1 Photograph of fatigue test specimens.

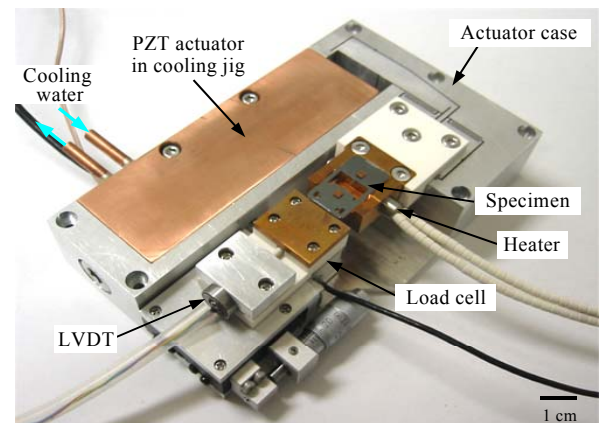


Fig. 2 Uniaxial tensile tester utilized for fatigue tests.

Table I Quasi-static tensile test results.

Specimen	Young's modulus E [GPa]	Fracture strength σ_f [GPa]	Fracture strain ϵ_f [%]
Single crystal silicon	1 169.2	3.41	2.02
	2 167.8	3.11	1.85
	3 169.4	3.27	1.93
	Average 168.8	3.26	1.93
Poly crystal silicon	1 157.0	2.10	1.34
	2 162.1	2.06	1.27
	3 163.2	2.09	1.28
	Average 160.8	2.08	1.30

All the fatigue tests were performed under controls of the actuator displacement and loading-unloading frequency in a tension-tension stress cycling mode with a triangle waveform. We determined the peak stress, σ_{peak} , during testing to be 10–90% of the average fracture strength, σ_f^{ave} , which was obtained from the quasi-static overload tests for each specimen, as listed in Table I.

3. Results and Discussions

Results of Cyclic Loading Tests

Figs. 3 show representative applied stress-time wave-

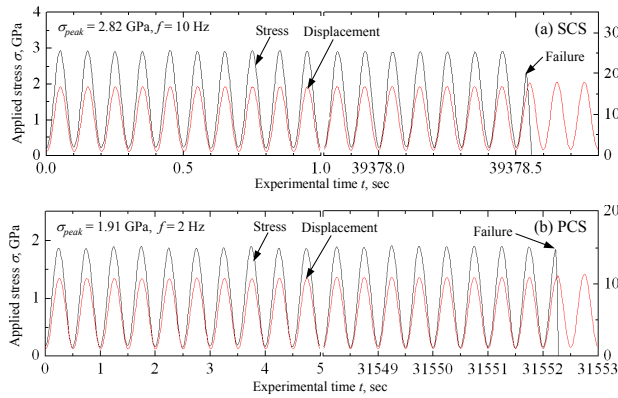


Fig. 3 Stress-time waveforms during fatigue tests.

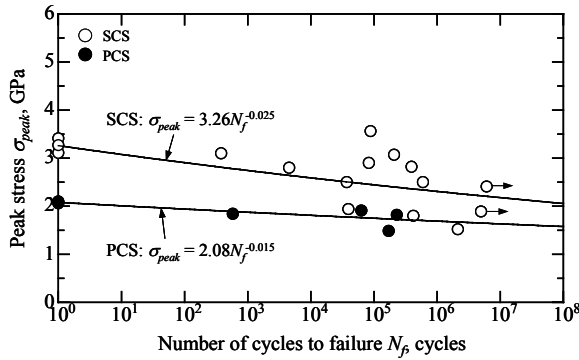


Fig. 4 S-N curves for SCS and PCS specimens.

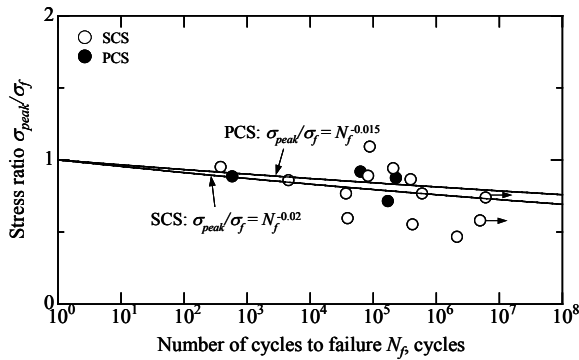


Fig. 5 Stress ratio vs. number of cycles to failure.

forms of (a) SCS and (b) PCS specimens. The stress-time waveform of the SCS specimen shows stable triangular waves indicating small frequency deviation. The peak stress and stress amplitude were also maintained constant throughout the test. An abrupt drop in the stress at 39,378.5 seconds is seen due to time-delayed fatigue failure. Waveform in the PCS specimen exhibits a trend similar as that in the SCS specimen.

S-N Curves

Fig. 4 shows the relationship between the applied peak stress, σ_{peak} , and the number of cycles to failure, N_f , in all the specimens tested. The fatigue life of each type of specimen increased with decreasing peak stress. Both the SCS and PCS specimens did not have a manifest fatigue limit, in that the S-N curves continue their downward trend at greater N_f values, though a few specimens did not fail even after megacycles.

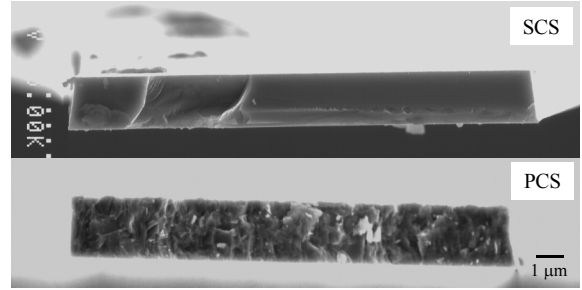


Fig. 6 Fracture surface of SCS and PCS specimens.

Fig. 5 depicts the ratio of applied peak stress to average fracture strength, $\sigma_{peak}/\sigma_f^{ave}$ versus the number of cycles to failure. The fatigue life of both the specimens has extended as the stress ratio parameter has decreased, as does σ_{peak} . Although the number of the PCS data is not enough, the scatter of the lifetime data in the SCS specimens is observed more than that in the PCS specimens. This indicates that the fatigue life of the PCS structure would be easily predicted than that of the SCS structure when these structures are subjected to fluctuation by an external force.

Fracture Surface

Fig. 6 show SEM photographs of fracture surface for the SCS and PCS specimens. The fracture surface of the SCS specimen formed a smooth inclined plane. Considering the surface angle, the inclined plane is thought to be $\{111\}$ cleavage planes for SCS with a diamond cubic structure. Fatigue crack nucleation probably occurred on the specimen surface, and the crack then continued to develop along an active $\{111\}$ cleavage plane. Fatigue failure of the SCS specimen strongly depends on a failure of the surface, in other words, the number of surface defects; so the large scatter of the life would have been observed. In contrast to the SCS specimen, the PCS specimen has an irregular fracture surface. Almost of crack nucleation occurred on the film inside, especially a grain boundary; therefore the small scatter of the life would have been produced.

4. Conclusions

We conducted pulsating tension fatigue tests of micro-scale SCS and PCS specimens. All the stress-time waveforms were constant throughout fatigue test. Fatigue life of SCS and PCS specimens extended as applied stress decreased, and the scatter of the life for SCS was bigger than that for PCS.

Acknowledgements

The authors would like to express sincere thanks to Micro-machine Center for preparing fatigue test specimens.

References

- [1] J. A. Connally and S. B. Brown, *Science*, **256**, (1992), p. 1537.
- [2] T. Namazu and Y. Isono, *Proc. of The 17th IEEE Int. Conf. on Microelectromech. Syst., MEMS 2004*, (2004), p. 149.
- [3] T. Namazu, S. Inoue, H. Takemoto, and K. Koterazawa, *IEEJ Trans. on Sens. and Micromach.*, **125**(9), (2005), p. 374.